Cyano-Halogen Interactions in [EDT-TTF-I]$_2$[Ni(mnt)$_2$] and [EDT-TTF-I$_2$]$_2$-[Ni(mnt)$_2$] and Geometrical Evolutions within Mixed-Valence or Fully Oxidized TTF Dyads

Thomas Devic,[a] Benoît Domercq,[b] Pascale Auban-Senzier,[c] Philippe Molinié,[b] and Marc Fourmigué*[a]

Keywords: Radical ions / S ligands / Magnetic properties / Crystal engineering / Non-covalent interactions

The structure of the iodo-substituted tetrathiafulvalene derivative EDT-TTF-I is described, with neutral molecules associated into inversion-centred dyads; no short intermolecular I···I contacts are observed. Electrocrystallisation of EDT-TTF-I (**1**) or EDT-TTF-I$_2$ (**2**) in the presence of [nBu$_4$N][Ni(mnt)$_2$] afforded 2:1 salts, formulated as [**1**]$_2$[Ni(mnt)$_2$] and [**2**]$_2$[Ni(mnt)$_2$]. In both salts the organic donor molecules **1** or **2** are associated into inversion-centred dyads, connected to the [Ni(mnt)$_2$] species through a short, directional CN···I interaction. The dyads alternate with the nickel dithiolene complex into mixed ...DDADDADDA... stacks. Comparisons in both salts of intramolecular bond lengths, intra-dyad overlap modes, and magnetic susceptibilities, indicate a full charge-transfer in [**1**]$_2$[Ni(mnt)$_2$], formulated as $[\mathbf{1}]_2^{2+}[\mathrm{Ni(mnt)_2}]^{2-}$, while a mixed-valence state is observed in $[\mathbf{2}]_2^{+\cdot}[\mathrm{Ni(mnt)_2}]^{-\cdot}$.

Introduction

Intermolecular CN···I interactions[1,2] have been known for a long time in the solid state chemistry of organic molecules[3] and were recently investigated theoretically.[4] Mainly associated with the most polarisable halogens (Br, I), they are characterised by a N···Hal distance far shorter than the sum of the van der Waals radii [N···I = 3.0−3.15 Å; Σ_{vdW}(N···I) = 3.53 Å] together with a strong tendency to linearity.[5,6] Recent ab initio intermolecular perturbation theory calculations showed that the attractive nature of the N···I interaction is mainly due to electrostatic effects while its directionality can be explained by the anisotropic electron distribution around the halogen atom.[4] This directional interaction has been used deliberately in the synthesis of several organic salts derived from iodinated tetrathiafulvalenes such as TTF-I,[7] EDT-TTF-I,[8,9] EDO-TTF-I$_2$,[10] or DIETS[11] and cyano-containing anions such as Ag(CN)$_2^-$, Pd(CN)$_4^{2-}$ or [Pd(mnt)$_2$]$^{2-}$. It is also elegantly used in a TTF molecule containing both a pyrazino and two iodo moieties,[12] or by the inclusion in the anionic layer of neutral iodinated molecules.[13] Among those various cyanide-containing counterions, only one example has been described which involves an open-shell anion, namely the [Ni(mnt)$_2$]$^{-\cdot}$ nickel dithiolene complex, in a 2:1 salt with EDO-TTF-I$_2$.[14] In this salt, the metallic conductivity is due to the one-dimensional chains of EDO-TTF-I$_2$, while the localised spins of the [Ni(mnt)$_2$]$^-$ anions behave as a one dimensional ferromagnet, and interact with conduction electrons. In a search for similar systems where localised and itinerant spins coexist and eventually interact,[15] we investigated the salts derived from the mono- and diiodo-substituted tetrathiafulvalene derivatives EDT-TTF-I (**1**) and EDT-TTF-I$_2$ (**2**) with the open-shell anion [Ni(mnt)$_2$]$^{-\cdot}$ and describe here their structural and electronic properties, paying special attention to the CN···I and the magnetic organic/inorganic interactions.

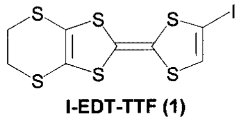

I-EDT-TTF (1)

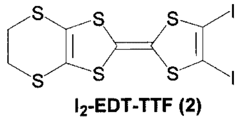

I$_2$-EDT-TTF (2)

---

[a] Laboratoire Chimie Inorganique, Matériaux et Interfaces, FRE 2447 CNRS-Université d'Angers, UFR Sciences,
Bât. K, 2 bd. Lavoisier, 49045 Angers, France
Fax: (internat.) + 33-241/735-405
E-mail: marc.fourmigue@univ-angers.fr

[b] Institut Jean Rouxel, CNRS-Université de Nantes,
2, rue de la Houssinière, BP32229, 44322 Nantes, France

[c] Laboratoire de Physique des Solides, UMR 8502 CNRS-Université Paris-Sud,
Bât. 510, 91405 Orsay cedex, France

1434−1948/02/1111−2844 $ 20.00+.50/0

Results and Discussion

Solid-State Structures

Compounds **1** and **2** were prepared as described previously[16] and recrystallised from toluene. Molecule **1**, in the neutral state, crystallises in the triclinic system, space group $P\bar{1}$ with two crystallographically independent molecules in the unit cell (Figure 1). One of these exhibits strong distortions from planarity with folding angles along the S···S hinge of the two dithiole rings of 14.3(1) and 14.0(1)° for the dithiole rings bearing the dithioethylene and iodo substituents, respectively. The other crystallographically independent molecule is almost planar,[17] except for the dithioethylene bridge, which is also disordered over two positions with a 55:45 distribution. The intramolecular bond lengths and angles differ only slightly from those observed in the unsubstituted EDT-TTF.[18] The molecules are associated into inversion-centred dyads with plane-to-plane distances of 3.43(2) and 3.51(2) Å in the two independent dyads, respectively, while the shortest intermolecular I···I contacts are observed at 4.47 Å, thus excluding the presence of I···I interactions in the solid state.[16,19,20] (NB The structure of the neutral diiodo derivative **2** could not be fully determined due to the poor quality of the crystals.[21]) Electrocrystallisation of **1** and **2** in the presence of [nBu$_4$N]-[Ni(mnt)$_2$] afforded in both cases a 2:1 salt, formulated as [**1**]$_2$[Ni(mnt)$_2$] and [**2**]$_2$[Ni(mnt)$_2$]. They crystallise in the triclinic system, space group $P\bar{1}$, and exhibit almost identical gross structural features (Figure 2 and 3), with the organic donor molecules **1** or **2** associated into inversion-centred dyads connected to the [Ni(mnt)$_2$] moiety through a short, directional CN···I interaction with the following characteristics: N···I = 2.926(4) Å, C≡N···I = 177.9(2)° in [**1**]$_2$[Ni(mnt)$_2$]; N···I = 2.949(9) Å, C≡N···I = 171.6(9)° in [**2**]$_2$[Ni(mnt)$_2$]. It should be stressed that the CN···I distances observed here are much shorter than the distances observed in the neutral *p*-iodobenzonitrile, for example (3.0−3.15 Å). This striking shortening suggests an enhanced interaction due to the electrostatic nature of the CN···I interaction. Indeed, in those systems where the iodine atom is covalently linked to the *cationic* tetrathiafulvalene and the nitrile group is part of an *anionic* dithiolene complex, this polarised interaction is expected to be enhanced, as observed here and in the salts of the iodinated TTF's mentioned above. Such an activation of iodinated molecules has also been performed by the incorporation of neighbouring electron-withdrawing fluorinated groups, leading to enhanced N···I interactions.[22,23] To further demonstrate the electrostatic character of this interaction, the *reverse polarisation*, which involves a cyanide-bound tetrathiafulvalene cation and halogenated anions, has recently been addressed:[24] the interaction was completely suppressed in these cases.

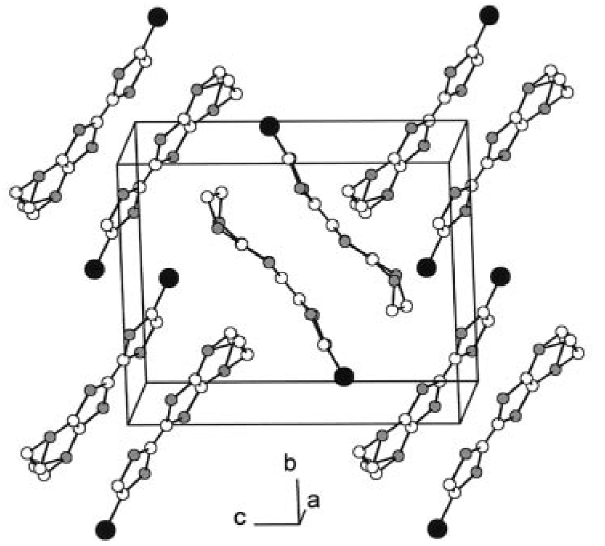

Figure 1. A view of the unit cell of neutral EDT-TTF-I (**1**); sulfur atoms are in dark grey, iodine atoms in black; note the folding of the dithiole rings of the molecule located at the centre of the unit cell

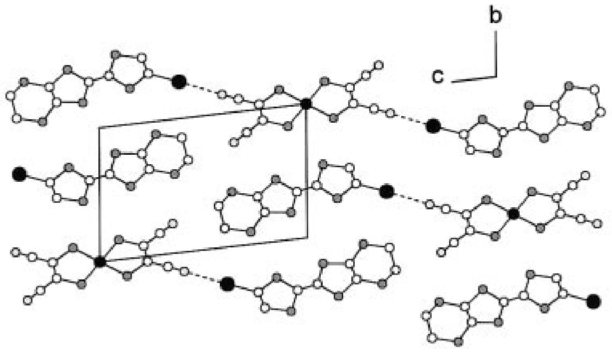

Figure 2. Projection view (along *a*) of a molecular plane in [**1**]$_2$[Ni(mnt)$_2$] showing the CN···I interaction (dotted line)

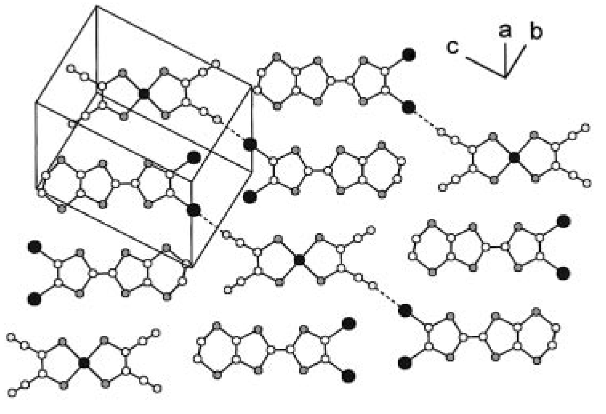

Figure 3. View of a molecular plane in [**2**]$_2$[Ni(mnt)$_2$] showing the CN···I interaction (dotted line)

In both salts, as shown in Figure 4, the oxidised donor molecules are associated into inversion-centred dyads which alternate with the nickel dithiolene complex into mixed ...DDADDADDA... stacks. This alternating structure is in sharp contrast with the EDO-TTF-I$_2$ salt described by Enoki et al.,[14] where segregated stacks were observed.

The magnetic susceptibilities of both salts, as determined from SQUID measurements, are very different (Figure 5).

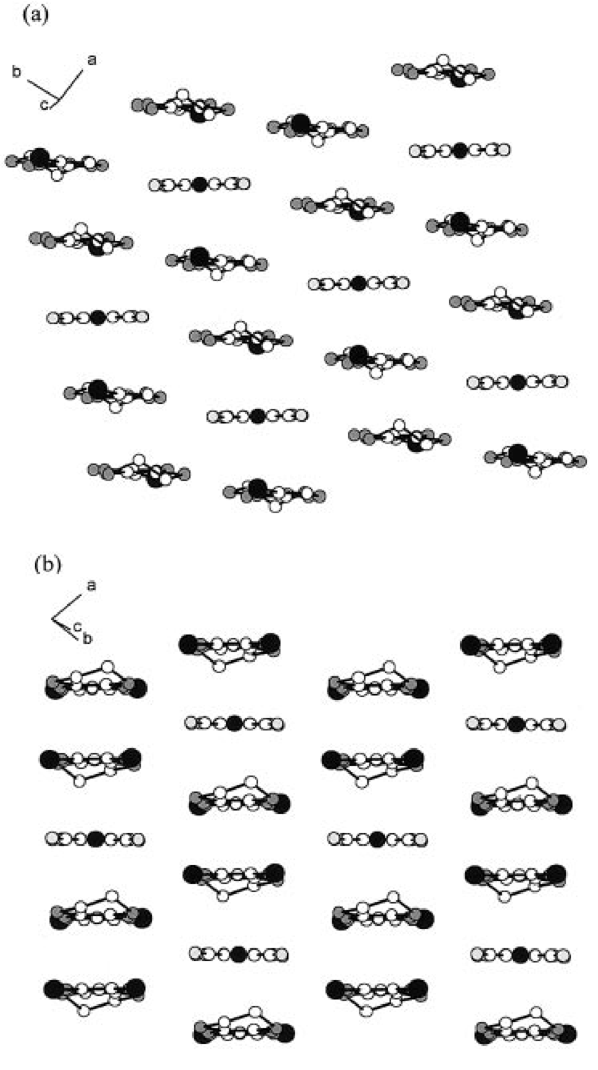

Figure 4. Views along the long molecular axis of the mixed ...DDADDADDA... chains arranged into slabs in [**1**]$_2$[Ni(mnt)$_2$] (a) and [**2**]$_2$[Ni(mnt)$_2$] (b)

Indeed, [**2**]$_2$[Ni(mnt)$_2$] follows a Curie−Weiss-type law, $\chi = C/(T\text{-}\theta)$, with $C = 0.71$ and $\theta = -8$ K — the signature of two localised, weakly interacting spin carriers — while [**1**]$_2$[Ni(mnt)$_2$] exhibits a weak paramagnetism (see below). Single crystal conductivity measurements performed on [**2**]$_2$[Ni(mnt)$_2$] show a semi-conducting behaviour with a low room-temperature conductivity ($\sigma_{RT} = 6 \times 10^{-3}$ S cm^{-1}) and an activation energy of 1700 K (0.14 eV).[25] These contrasting behaviours raise several questions concerning the actual oxidation state of both the donor molecules and the nickel dithiolene complex in the two salts. A precise examination of the two structures and their differences is expected to reveal the actual nature of these salts. Are we in presence of mixed-valence organic dyads, $[\mathbf{1}]_2^{+\cdot}$ or $[\mathbf{2}]_2^{+\cdot}$, together with a paramagnetic $[\mathrm{Ni(mnt)_2}]^{-\cdot}$ radical anion, or in the presence of fully oxidised donor molecules, $[\mathbf{1}]_2^{2+}$ or $[\mathbf{2}]_2^{2+}$ with the reduced diamagnetic $[\mathrm{Ni(mnt)_2}]^{2-}$ complex?

A comparison of the redox potentials favours the mixed-valence solution. Indeed, as shown in Scheme 1, both donor

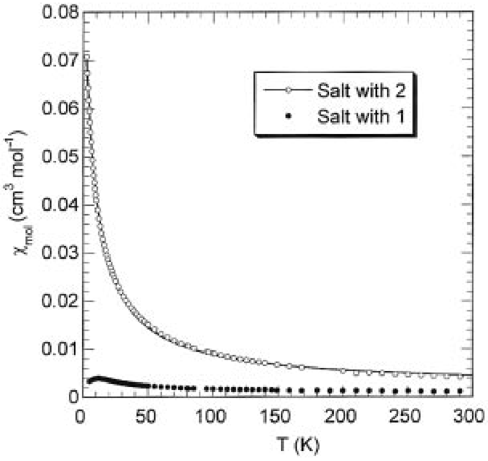

Figure 5. Temperature dependence of the magnetic susceptibility in [**1**]$_2$[Ni(mnt)$_2$] and [**2**]$_2$[Ni(mnt)$_2$]; the solid line for [**2**]$_2$[Ni(mnt)$_2$] is the fit to the Curie−Weiss model, $\chi_{mol} = \chi_0 + C/(T - \theta)$, with $\chi_0 = 0.002$ cm^3·mol^{-1}, C = 0.71 cm^3·K·mol^{-1} and $\theta = -8$ K

molecules oxidise at potentials far above the $\mathrm{Ni(mnt)_2^{2-/1-}}$ couple, and **1** oxidises at a slightly lower potential than **2**, illustrating the electron-withdrawing effect of the iodine atom. The evolution of the bond lengths within the donor molecules and the dithiolene complexes is also a very efficient tool for evaluating the degree of charge transfer. As observed in Table 1, the lengthening of the central C=C bond and shortening of the C−S bonds within the TTF cores upon oxidation is observed to a larger extent in [**1**]$_2$[Ni(mnt)$_2$] than in [**2**]$_2$[Ni(mnt)$_2$]. Similarly, the bond lengths' evolution within the Ni(mnt)$_2$ complex in both salts (Table 2) more clearly reveals that the monoanionic[26] $\mathrm{Ni(mnt)_2^{-\cdot}}$ is present in [**2**]$_2$[Ni(mnt)$_2$], while most probably the dianionic $\mathrm{Ni(mnt)_2^{2-}}$ moiety[27] is found in [**1**]$_2$[Ni(mnt)$_2$]. This assignment is further confirmed by the ν_{CN} stretching frequency (Table 2). We are therefore faced here with two totally different electronic distributions: mixed-valence organic $[\mathbf{2}]_2^{+\cdot}$ dyads alternating with an anionic $[\mathrm{Ni(mnt)_2}]^{-\cdot}$ moiety in [**2**]$_2$[Ni(mnt)$_2$], and dicationic $[\mathbf{1}]_2^{2+}$ dyads alternating with a dianionic $[\mathrm{Ni(mnt)_2}]^{2-}$ moiety in [**1**]$_2$[Ni(mnt)$_2$].

Besides the intramolecular bond length variations, this electronic distribution is also reflected in the overlap geometry within the organic dyads. Indeed, as shown in Figure 6, the overlap interaction between two donor molecules within a dyad in [**1**]$_2$[Ni(mnt)$_2$] is of the eclipsed type, with a short plane-to-plane distance at 3.396(1) Å, characteristic of a fully oxidized $[\mathbf{1}]_2^{2+}$ dyad. The eclipsed configuration indeed favours the best overlap between SOMOs and, as a consequence, the pairing of the two spin carriers in their bonding combination. The corresponding calculated $\beta_{\mathrm{HOMO\cdots HOMO}}$ overlap interaction amounts to 1.03 eV, a large value which also confirms the dicationic character of the dyad. On the other hand, a so-called bond-over-ring overlap is observed in the dyads in [**2**]$_2$[Ni(mnt)$_2$] together with a larger plane-to-plane distance [3.418(1) Å] and a much reduced $\beta_{\mathrm{HOMO\cdots HOMO}}$ overlap interaction

Table 2. Characteristic averaged bond lengths (Å) and ν_{CN} IR band (cm^{-1}) in Ni(mnt)$_2^x$ ($x = -2, -1$) in different salts

	x	Ni−S bonds	C−S bonds	C=C bonds	ν_{CN}	Ref.
$[Et_4N]_2[Ni(mnt)_2]$	−2	2.174(2)	1.742(5)	1.35(1)	2191	27
$[\mathbf{1}]_2[Ni(mnt)_2]$	−2	2.171(1)	1.731(4)	1.362(6)	2191	this work
$[\mathbf{2}]_2[Ni(mnt)_2]$	−1	2.142(2)	1.723(9)	1.369(11)	2204	this work
$[Et_4N][Ni(mnt)_2]$	−1	2.147(3)	1.720(10)	1.369(12)	2207	26

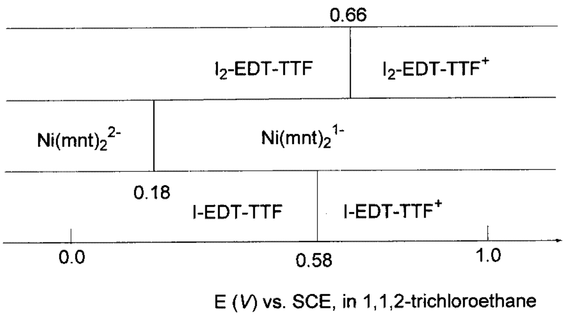

Scheme 1

Table 1. Characteristic bond lengths in the donor molecules, in various oxidation states

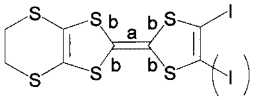

	ρ	C=C bond (a)	C−S bonds (b)	ref.
EDT-TTF-I (**1**)	0	1.332(8)	1.763(7)	this work
$[\mathbf{1}]_2[Ag(CN)_2]$	0.5	1.369(4)	1.736(4)	9
$[\mathbf{1}]_2[Ni(mnt)_2]$	0.5	1.382(6)	1.723(4)	this work
$[\mathbf{2}]_2[I_3]$	0.5	1.365(10)	1.741(8)	16
$[\mathbf{2}]_2[Ni(mnt)_2]$	1	1.389(11)	1.731(9)	this work
$[\mathbf{2}][I_3]$	1	1.40(2)	1.718(9)	unpubl. results

(0.435 eV) — another confirmation of its mixed-valence character. Note also that the calculated β values for the interactions between the mixed-valence dyads are much smaller albeit not negligible (≈ 40 meV).

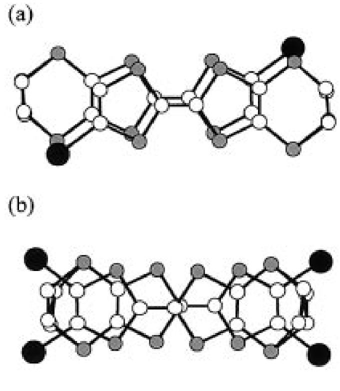

Figure 6. The overlap within each donor dyad in $[\mathbf{1}]_2[Ni(mnt)_2]$ (a) and $[\mathbf{2}]_2[Ni(mnt)_2]$ (b)

All these results confirm the above-mentioned formulations, i.e. a full charge-transfer in $[\mathbf{1}]_2^{2+}[Ni(mnt)_2]^{2-}$ and a mixed-valence state in $[\mathbf{2}]_2^{+\cdot}[Ni(mnt)_2]^{-\cdot}$. A fully oxidised dyad has already been observed in $[TTF\text{-}I]_2[Pd(mnt)_2]$, a similar system described by Bryce et al. with a closely related structure and CN··I interaction.[7] In this salt, TTF-I is more easily oxidised than **1** while $[Pd(mnt)_2]^{2-}$ oxidises at higher potentials than $Ni(mnt)_2^{2-}$. It is therefore understandable that this salt was formulated as $[TTF\text{-}I]_2^{2+}[Pd(mnt)_2]^{2-}$. The same formulation in $[\mathbf{1}]_2^{2+}[Ni(mnt)_2]^{2-}$ appears more surprising given the potential difference between the two redox centres (−0.40 V, Scheme 1). Furthermore, from the $[TTF\text{-}I]_2^{2+}[Pd(mnt)_2]^{2-}$ and $[\mathbf{1}]_2^{2+}[Ni(mnt)_2]^{2-}$ formulations, one would expect a fully diamagnetic behaviour, in contrast to the temperature dependence of the magnetic susceptibility in both salts. $[TTF\text{-}I]_2^{2+}[Pd(mnt)_2]^{2-}$ was indeed reported to behave as a one-dimensional Heisenberg chain with an isotropic nearest-neighbour exchange interaction of $J \approx -50$ K. The temperature dependence of the magnetic susceptibility in $[\mathbf{1}]_2[Ni(mnt)_2]$ (Figure 5) shows a similar shape even though the fits we performed with the Bonner−Fisher model[28] are consistent with a J value of −18 K but with a contribution of only 0.25 mol of $S = 1/2$, a behaviour which we cannot explain at present, although one possibility would be the contribution of a sizeable TIP arising from the inorganic moiety. However, a control susceptibility measurement performed on $[Et_4N]_2[Ni(mnt)_2]$ confirmed the diamagnetic character of the dianionic $[Ni(mnt)_2]^{2-}$ component with a χ_{mol} value of -340×10^{-6} cm^3·mol^{-1}, attributable to the diamagnetic contribution of the different atoms, as evaluated from the Pascal constants (-290×10^{-6} cm^3·mol^{-1}). This observation of a paramagnetic contribution in Bryce's $[TTF\text{-}I]_2[Pd(mnt)_2]$ complex as well as in $[\mathbf{1}]_2[Ni(mnt)_2]$ could also originate from a minority polymorph. However, an X-ray powder diagram of the polycrystalline sample used for the magnetic susceptibility measurements confirmed the identity of $[\mathbf{1}]_2[Ni(mnt)_2]$ as determined from the single-crystal diffraction experiment.

The observation of a mixed-valence salt in $[\mathbf{2}]_2[Ni(mnt)_2]$ is confirmed by the SQUID magnetic susceptibility, which shows that both paramagnetic entities, the $[\mathbf{2}]_2^{+\cdot}$ dyad and the $[Ni(mnt)_2]^{-\cdot}$ complex, contribute to the susceptibility, hence the Curie−Weiss law for two almost-independent spin carriers. The weak, negative θ value (−8 K) found in the temperature dependence of the magnetic susceptibility of $[\mathbf{2}]_2[Ni(mnt)_2]$ cannot find its origin in a ZFS of the nickel complex since the $[Ni(mnt)_2]^{-\cdot}$ moieties have a spin of 1/2; it must therefore stem from weak intermolecular interactions between the $[\mathbf{2}]_2^{+\cdot}$ moieties since the $[Ni(mnt)_2]^{-\cdot}$ moieties are fully isolated from each other in the structure. Indeed, as mentioned above, the calculated $\beta_{HOMO\cdots HOMO}$ overlap interaction between donor molecules pertaining to neighbouring dyads amounts to approximately 40 meV and can explain the Curie−Weiss behaviour observed here. Preliminary EPR measurements at room temperature performed on a polycrystalline sample of $[\mathbf{2}]_2[Ni(mnt)_2]$ show a single asymmetric line centred at $g = 2.032$ with a ΔH value of 240 G (Figure 7). Taking into account the presence of two types of spin carriers in the salt, the line can be tentatively decomposed as the sum of two lines of equal intensity, centred at the g values of 2.012 and 2.062. These values compare favourably with those reported in the literature for similar TTF dyads ($g = 2.005-2.008$)[29] and for $[Ni(mnt)_2]^{-\cdot}$ ($g = 2.0633$).[30]

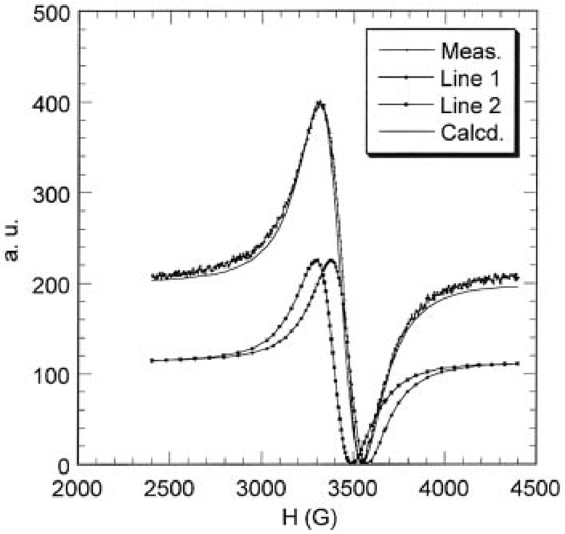

Figure 7. EPR signal obtained for $[\mathbf{2}]_2[Ni(mnt)_2]$; the solid line is the sum of the line 1 and line 2 components

Experimental Section

Synthesis: The donor molecules **1** and **2** were prepared as previously described. Electrocrystallization experiments were performed in two-compartment cells in 1,1,2-trichloroethane (10 mL) with $[nBu_4N][Ni(mnt)_2]$ (20 mg) as electrolyte and **1** or **2** (4 mg). Crystals were obtained on the anode after galvanostatic electrolysis (0.25 μA, 16 days for **1** and 0.5 μA, 12 days for **2**).

Crystallography: Details of the data collection and structure refinement are given in Table 3. For neutral **1** and $[\mathbf{1}]_2[Ni(mnt)_2]$ data were collected on a Stoe-IPDS or an Enraf−Nonius Mach3 diffractometer at 293 K with graphite-monochromatized Mo-K_α radiation ($\lambda = 0.71073$ Å). The Stoe software was used for data collection and reduction, and numerical absorption correction using crystal faces. For $[\mathbf{2}]_2[Ni(mnt)_2]$ data were collected on an Enraf−Nonius Mach 3 diffractometer, reduction of the data was performed with XCAD4 (Harms, 1986) and absorption correction from a ψ-scan (SHELXPREP). The structures were solved by direct methods (SHELXS-86) and refined using SHELXL. All atoms were refined anisotropically except hydrogen atoms and some carbon atoms of the disordered ethylene bridge (C15B in neutral **1**, C7, C7′, C8, C8′ in $[\mathbf{1}]_2[Ni(mnt)_2]$ and $[\mathbf{2}]_2[Ni(mnt)_2]$). Hydrogen atoms were introduced at calculated positions (riding model) and not refined. Crystallographic data (excluding structure factors) for the structures reported in this paper have been deposited with the Cambridge Crystallographic Data Centre as supplementary publication no. CCDC-178087, -178088 and -178089 for **1**, $[\mathbf{1}]_2[Ni(mnt)_2]$ and $[\mathbf{2}]_2[Ni(mnt)_2]$ respectively. Copies of the data can be obtained free of charge on application to CCDC, 12 Union road, Cambridge CB2 1EZ, UK [Fax: (internat.) +44-1223/336-033; E-mail: deposit@ccdc.cam.ac.uk].

Table 3. Crystallographic data

Formula	EDT-TTF-I (**1**) $C_8H_5IS_6$	$[\mathbf{1}]_2[Ni(mnt)_2]$ $C_{12}H_5IN_2Ni_{0.5}S_8$	$[\mathbf{2}]_2[Ni(mnt)]$ $C_{24}H_8I_4N_4NiS_{16}$
Formula mass	420.38	589.92	1431.61
Crystal system	triclinic	triclinic	triclinic
Space group	$P\bar{1}$	$P\bar{1}$	$P\bar{1}$
a/ Å	6.4507(7)	7.7632(16)	8.3183(10)
b/ Å	12.6268(15)	8.8071(18)	9.6862(10)
c/ Å	16.197(2)	13.951(3)	12.8455(10)
α/degrees	89.662(15)	94.52(3)	85.657(10)
β/degrees	84.568(15)	104.80(3)	80.218(10)
γ/degrees	79.988(15)	95.25(3)	80.595(10)
V/ Å^3	1293.2(3)	913.2(3)	1005.01(18)
Z	4	2	1
d_{calc}/g cm^{-3}	2.159	2.145	2.365
μ/mm^{-1}	3.408	3.165	4.414
Data collected	12511	8957	4049
Abspt. corr.	numerical	numerical	psi-scan
T_{min}, T_{max}	0.594, 0.725	0.657, 0.952	0.327, 0.451
Ind. data	4600	3311	3867
R_{int}	0.0883	0.0425	0.0129
Obs. data $[I > 2\sigma(I)]$	3175	2460	2867
Param. refined	285	213	222
$R(F)$	0.0496	0.0284	0.0390
$wR(F^2)$	0.1238	0.0608	0.1732
Residual d/e·Å^{-3}	1.6, −1.0	1.0, −0.35	0.87, −0.78.

Magnetic Measurements: Magnetic susceptibility measurements were performed on a Quantum Design MPMS5 SQUID magnetometer operating in the range 5−300 K with polycrystalline samples. Data were corrected for Pascal diamagnetism and sample holder contribution. Room temperature EPR measurements were obtained from a Bruker ER200D spectrometer operating in X-band (9.782 GHz) with a modulation of 1.25 G.

---

[1] O. Hassel, *Mol. Phys.* **1958**, *1*, 241−246.
[2] O. Hassel, C. Romming, *Q. Rev. Chem. Soc.* **1962**, *16*, 1−18.
[3] D. Britton, *Persp. Struct. Chem.* **1967**, *1*, 109−171.
[4] J. P. M. Lommerse, A. J. Stone, R. Taylor, F. H. Allen, *J. Am. Chem. Soc.* **1996**, *18*, 3108−3116.
[5] G. R. Desiraju, R. L. Harlow, *J. Am. Chem. Soc.* **1989**, *111*, 6757−6764.
[6] A. S. Batsanov, M. R. Bryce, A. Chesney, J. A. K. Howard, D. E. John, A. J. Moore, C. L. Wood, H. Gershtenman, J. Y. Becker, V. Y. Khodorkovsky, A. Ellern, J. Bernstein, I. F. Perepichka, V. Rotello, M. Grey, A. O. Cuello, *J. Mater. Chem.* **2001**, *11*, 2181−2191.
[7] A. S. Batsanov, A. J. Moore, N. Roberston, A. Green, M. R. Bryce, J. A. K. Howard, A. E. Underhill, *J. Mater. Chem.* **1997**, *7*, 387−389.

[8] T. Imakubo, H. Sawa, R. Kato, *J. Chem. Soc., Chem. Commun.* **1995**, 1097−1098.

[9] T. Imakubo, H. Sawa, R. Kato, *Synth. Metals* **1997**, *86*, 1847−1848.

[10] Y. Kuwatani, E. Ogura, H. Nishikawa, I. Ikemoto, M. Iyoda, *Chem. Lett.* **1997**, 817−818.

[11] T. Imakubo, H. Sawa, R. Kato, *J. Chem. Soc., Chem. Commun.* **1995**, 1667−1668.

[12] T. Imakubo, T. Maruyama, H. Sawa, K. Kobayashi, *Chem. Commun.* **1998**, 2021−2022.

[13] H. M. Yamamoto, J.-I. Yamaura, R. Kato, *J. Am. Chem. Soc.* **1998**, *120*, 5905−5913.

[14] J. Nishijo, E. Ogura, J. Yamaura, A. Miyazaki, T. Enoki, T. Takano, Y. Kuwatani, M. Iyoda, *Solid State Commun.* **2000**, *116*, 661−664.

[15] E. Coronado, J. R. Galan-Mascaros, C. J. Gomez-Garcia, V. Laukhin, *Nature* **2000**, *408*, 447−449 and references therein.

[16] B. Domercq, T. Devic, M. Fourmigué, P. Auban-Senzier, E. Canadell, *J. Mater. Chem.* **2001**, *11*, 1570−1575.

[17] The corresponding folding angles of the dithiole rings amount to 4.8(1) and 1.7(2)°.

[18] B. Garreau, D. De Montauzon, P. Cassoux, J.-P. Legros, J.-M. Fabre, K. Saoud, S. Chakroune, *New. J. Chem.* **1995**, *19*, 161−171.

[19] G. R. Desiraju, R. Parthasarathy, *J. Am. Chem. Soc.* **1989**, *111*, 8725−8726.

[20] S. L. Price, A. J. Stone, J. Lucas, R. S. Rowland, A. E. Thornley, *J. Am. Chem. Soc.* **1994**, *116*, 4910−4918.

[21] Compound **2** crystallises in the orthorhombic system with a = 12.6757(13), b = 13.8122(9), c = 16.4095(13) Å, V = 2873.0(7) Å^3.

[22] E. Corradi, S. V. Meille, M. T. Messina, P. Metrangolo, G. Resnati, *Angew. Chem. Int. Ed.* **2000**, *39*, 1782−1786.

[23] R. B. Walsh, C. W. Padgett, P. Metrangolo, G. Resnati, T. W. Hanks, W. T. Pennington, *Cryst. Growth Des.* **2001**, *1*, 165−175.

[24] T. Devic, J. N. Bertran, B. Domercq, E. Canadell, N. Avarvari, P. Auban-Senzier, M. Fourmigué, *New J. Chem.* **2001**, *25*, 1418−1424.

[25] No reliable conductivity data could be obtained from [**1**]$_2$[Ni(mnt)$_2$] as the crystals were too small.

[26] A. Kobayashi, Y. Susuki, *Bull. Chem. Soc. Jpn.* **1977**, *50*, 2650−2656.

[27] C. Mahadevan, M. Seshasayee, A. Radha, P. T. Manoharan, *Acta Crystallogr., Sect. C* **1984**, *40*, 2032−2034.

[28] O. Kahn, in *Molecular Magnetism*, VCH, Weinheim, 1993, ch. 11.

[29] A. Dolbecq, M. Fourmigué, P. Batail, C. Coulon, *Chem. Mater.* **1994**, *6*, 1413−1418 and references therein.

[30] A. Davison, N. Edelstein, R. H. Holm, A. H. Maki, *Inorg. Chem.* **1963**, *2*, 1227−1232.

Received January 28, 2002
[I02045]